2008

A Dual Siso Controller for a Vapor Compression Refrigeration System

Jackson Braz Marcinichen
Federal University of Santa Catarina

Thiago N. del Holanda
Federal University of Santa Catarina

Claudio Melo
Federal University of Santa Catarina

A DUAL SISO CONTROLLER FOR A VAPOR COMPRESSION REFRIGERATION SYSTEM

Jackson B. MARCINICHEN, Thiago N. HOLANDA, Cláudio MELO
POLO Research Laboratories for Emerging Technologies in Cooling and Thermophysics
Department of Mechanical Engineering, Federal University of Santa Catarina
P.O. Box 476, 88040-900, Florianópolis, SC, BRAZIL
Phone: +55 48 3234 5691, e-mail: melo@polo.ufsc.br

ABSTRACT

This study investigates the use of a dual SISO (*Single Input, Single Output*) control strategy for the simultaneous control of compressor speed and expansion valve opening. The experimental work was carried out using a purpose-built test facility (a breadboard refrigeration system) consisting of a variable speed compressor (VSC), an electric expansion valve (EEV), a secondary flow rate and temperature controlled water loop (condensing medium), and a secondary flow rate and temperature controlled brine loop (cooling medium). The control strategy was devised to obtain a maximum system coefficient of performance (*COP*) within a cooling capacity range of 300 to 800 Watts. The refrigeration system was identified using the step-response method, which provided first-order linear models for both the evaporator superheat and the brine exit temperature. The models were used to derive two PI (*Proportional-Integral*) controllers, one for the evaporator superheat as a function of the EEV opening and another for brine exit temperature as a function of the compressor speed. The EEV controller was developed based on the so-called root locus method, whilst the VSC controller was designed based on the well-known Ziegler-Nichols method. Both controllers were implemented into a dual SISO control strategy that operated very satisfactorily.

1. INTRODUCTION

Due to the growth of the electronics field and also to the increasing demands for energy conservation, some conventional components of vapor compression refrigeration systems are gradually being replaced. For example, single speed compressors and capillary tubes are being replaced in some systems by variable speed compressors (VSC) and electric expansion valves, respectively. Such new components allow the development of smart control strategies not only to save energy but also to reduce fluctuations in the compartment temperatures.

Tassou and Qureshi (1996) showed that cooling capacity control is vital in decreasing the energy consumption of refrigeration systems. Cooling capacity control reduces the compressor cyclic thermodynamic losses and improves the system efficiency in steady-state regime due to the smaller pressure difference acting on the compressor under partial thermal load conditions. The authors also showed a comparison among several methods of cooling capacity control: on/off, hot gas by-pass, suction pressure control, compressor speed variation, etc. According to these authors, the most energy efficient technique is that based on the compressor speed variation. Comments on the importance of using variable opening expansion devices in refrigeration systems were made by Tassou and Qureshi (1996) and by Shimma *et al*. (1988), but none of these researchers carried out any systematic study on the subject.

Outtagarts *et al*. (1997) studied the effect of an EEV on the thermodynamic performance of a refrigeration system. Two valve controllers were designed, a PD (*Proportional-Derivative*) and an OQR (*Optimal Qualitative Regulation*), both with gain scheduling and response to the evaporator superheat. The behavior of the EEV system was compared to those with three distinct thermostatic expansion valves (TEV), under disturbances in the compressor speed. The authors found that with the EEV the evaporator superheat stabilized in a time period 4 to 14 times shorter than that required when any of the TEVs were used. They also found that in a steady-state regime the EEV maintained the superheating at the set-point value, independently of compressor speed and controller type. Such behavior was not observed with the TEVs, since the superheating varied with the evaporating pressure and compressor speed.

Wu *et al*. (2005) implemented a dual SISO control strategy in an air conditioned system composed of an EEV and a VSC. PID (*Proportional-Integral-Derivative*) controllers and a self-tuning fuzzy algorithm were developed to control the suction pressure through the compressor speed and the room temperature through the expansion valve

opening. Controllability tests were carried out, showing that the adopted control strategy provided an effective control of the room temperature.

This study explores the use of a dual SISO control strategy in a refrigeration system comprised of a VSC, an EEV and two-flow rate and temperature controlled secondary heat transfer loops. The aim was to maximize the system coefficient of performance (*COP*), both under steady-state and transient conditions and within a cooling capacity range of 300W to 800W. Each controller was designed using a PI control structure.

It should be mentioned that in a previous study carried out with the same testing facility, Pöttker and Melo (2006) showed that in a steady-state regime and with a fixed refrigerant charge there was an optimum combination of compressor speed and valve opening that maximized the *COP*. They also concluded that there was an optimum refrigerant charge for each compressor speed and valve opening combination.

2. EXPERIMENTAL SETUP

The experimental apparatus was essentially an R-134a vapor compression refrigeration loop. Figure 1 shows a schematic representation of the testing facility. A hermetic 10.61cm^3 displacement reciprocating compressor, with a speed range of 1800rpm to 4500rpm, was used to drive the refrigerant flow.

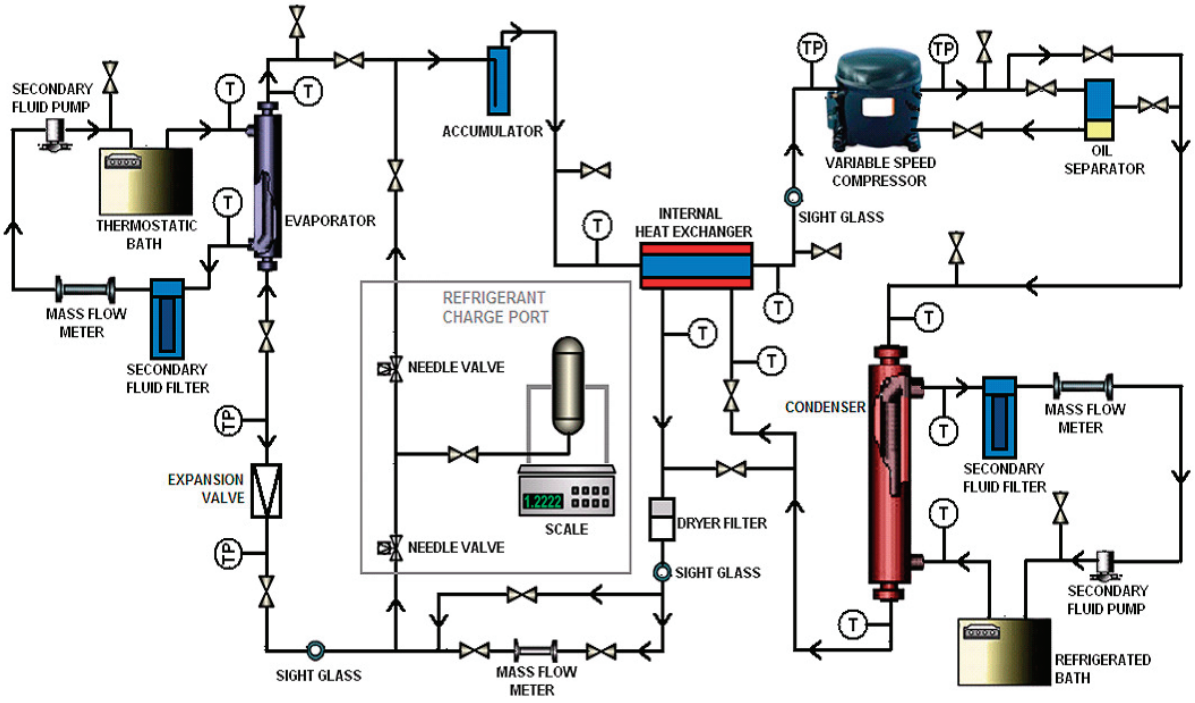

Figure 1: Experimental apparatus

The condenser and the evaporator, both of the tube-in-tube type, were connected to two secondary heat transfer circuits whose temperatures were controlled by a thermostatic bath on the evaporator side and by a refrigerated bath on the condenser side. The secondary fluid flows were regulated by variable speed pumps. Brine of 27% ethylene-glycol aqueous solution was used for the evaporator. Pure water was used for the condenser.

The expansion device was a PWM (*Pulse Width Modulated*) EEV, with a duty cycle ranging from 0 to 100% and with an orifice diameter of 0.397mm. A liquid line/suction line heat exchanger was used to increase the refrigerant subcooling at the valve inlet. The refrigerant charge was kept at 560g.

The condenser and evaporator heat transfer rates were obtained from energy balances on the refrigerant and secondary fluid sides. The refrigerant heat transfer rate was calculated by multiplying the R-134a mass flow rate,

measured by a Coriolis mass flow meter, by the enthalpy difference between the heat exchanger inlet and outlet. Immersion T-type thermocouples (T) and pressure transducers (P) were installed at selected points of the circuit to calculate the refrigerant enthalpies and the evaporator superheat. The secondary fluid heat transfer rate was calculated using the volumetric flow rate, measured by a turbine flow meter, the fluid density, the specific heat and the temperature difference between the heat exchanger inlet and outlet. For most of the tests the difference between the refrigerant-side and the secondary fluid-side heat transfer rates was less than 2%, for both heat exchangers. The coefficient of performance was calculated by dividing the brine heat transfer rate by the input power. A control and data acquisition system was used to monitor the experimental variables and to set the compressor speed and valve opening.

3. EEV CONTROLLER

The first controller action is to modulate the expansion valve opening (A_{EEV}) in order to maintain the evaporator superheat (T_{SH}) at the set-point value ($T_{SH,REF}$). Figure 2 illustrates such a controller through a block diagram

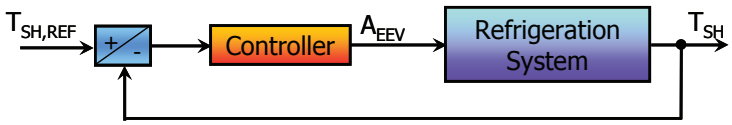

Figure 2: EEV controller

3.1 System identification and controller design

The system identification process has the objective of deriving a mathematical model capable of representing the dynamic behavior of the system under study. A linear first-order model with delay was used to correlate T_{SH} with the A_{EEV} variations. The superheating was calculated from the refrigerant temperature difference between the liquid accumulator exit and the evaporator inlet. Equations 1 and 2 show the model in the time and Laplace domains, respectively.

$$\tau \frac{dy(t)}{dt} + y(t) = K_P u(t - \theta) \tag{1}$$

$$G(s) = \frac{y(s)}{u(s)} = \frac{K_P e^{-\theta s}}{\tau s + 1} \tag{2}$$

The input (u) and output (y) parameters are A_{EEV} and T_{SH}, respectively. G is the transfer function, τ the system time constant, K_P the gain and θ the transport delay.

The model parameters were obtained varying the EEV opening from 48% to 52%. The compressor speed and the condenser and evaporator bath temperatures were maintained at 3600rpm, 35.0°C and 9.9°C, respectively. The volumetric flow rates of the secondary loops were established at 1.20L/min. These operation conditions are from now on referred as the *standard conditions*.

The K_P, τ and θ values were estimated in order to minimize the difference between the model predictions and the experimental data. For this controller θ was disregarded and K_P and τ were estimated as -1.3°C/% and 95s, respectively. Figures 3 and 4 depict a part of the identification test, showing the T_{SH} response to a step change in the A_{EEV} and also the T_{SH} model predictions against the experimental data.

Hong *et al*. (1992) showed that linear first-order models were able to represent the dynamics of the evaporator superheat and that a PI structure was suitable to control the fluid flow along the evaporator. Additionally, it is well known that the PI structure is characterized by its simplicity and capacity to establish an offset zero for reference tracking and disturbance rejection. The option of the PI structure was then selected for this study. Equation 3 shows the PI controller transfer function in the Laplace domain.

$$C(s) = K_C(1 + \frac{1}{T_I s}) \quad (3)$$

The controller was designed according to the root locus method in order to generate a system settling time of 52s and a T_{SH} maximum overshoot of 10%. The T_I and K_C parameters were calculated as 25s and -10%/°C, respectively.

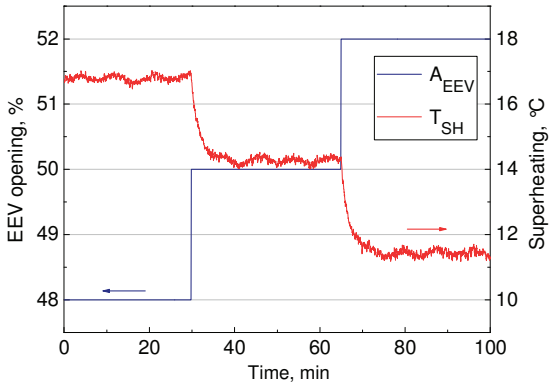

Figure 3: EEV - model identification

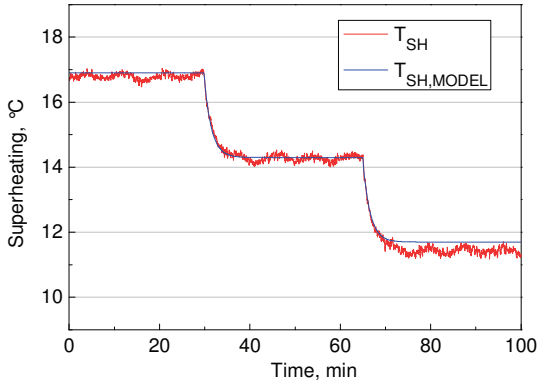

Figure 4: EEV - experimental vs. prediction

3.2 Controller evaluation

Tracking tests were carried out with the experimental apparatus running under the standard operation conditions to evaluate the controller performance. Figures 5 and 6 show that the controller increased the valve opening in response to a drop in the T_{SH} reference value. It can be noted that the controller worked as expected, with a settling time of 70s, closer to the designed value.

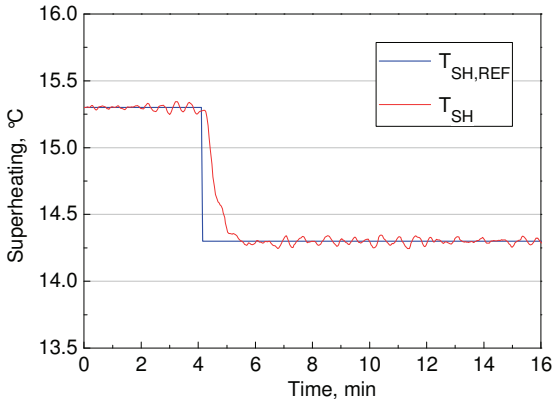

Figure 5: $T_{SH,REF}$ variation

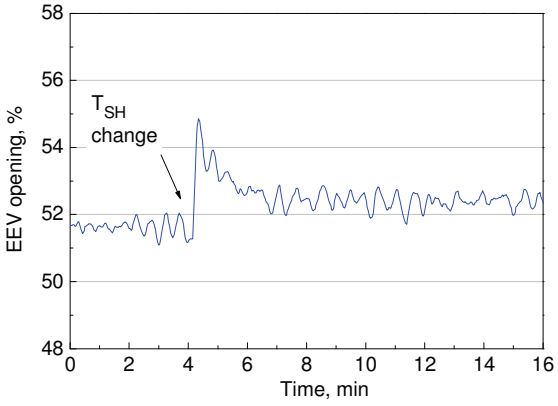

Figure 6: A_{EEV} variation

4. VSC CONTROLLER

The second controller action is to vary the compressor speed (N_{COMP}) in order to maintain the brine exit temperature (T_R) at a pre-defined value. Figure 7 illustrates such a controller through a block diagram.

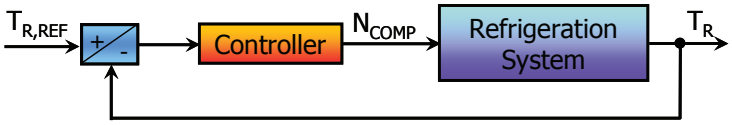

Figure 7: VSC controller

4.1. System identification and controller design

The experimental apparatus was firstly set at the standard operation conditions, with N_{COMP} and A_{EEV} set at 4200rpm and 50%, respectively. Next, step changes of 600rpm were applied to N_{COMP} and the T_R behavior was evaluated over time. The system was identified using the linear model given in equation 2, where the input (u) and output (y) parameters now stand for N_{COMP} and T_R, respectively. The model parameters, K_P, τ and θ, were then calculated as -0.007°C/rpm, 4s, and 4s, respectively.

This controller was also developed based on the PI structure, given in equation 3. The controller parameters were adjusted according to the Ziegler-Nichols (1942) method. With such an analytical method the controller parameters are calculated from the identified model parameters, as shown in equation 4. As a result the following values were obtained for K_C and T_I: -1285rpm/°C and 12.5s.

$$a = \frac{K_P \theta}{\tau}, \quad K_C = \frac{0.9}{a}, \quad T_I = 3\theta \tag{4}$$

4.2. Controller evaluation

Reference tracking tests were also carried out with the experimental apparatus running under the standard operation conditions, with a valve opening of 50% and under a $T_{R,REF}$ step change of 2.2°C to 3.2°C, to evaluate the controller performance.

Figures 8 and 9 show the variations of the brine exit temperature (T_R), cooling capacity (Q_{EVAP}), and compressor speed (N_{COMP}), as a result of a step change in the brine temperature reference value ($T_{R,REF}$).

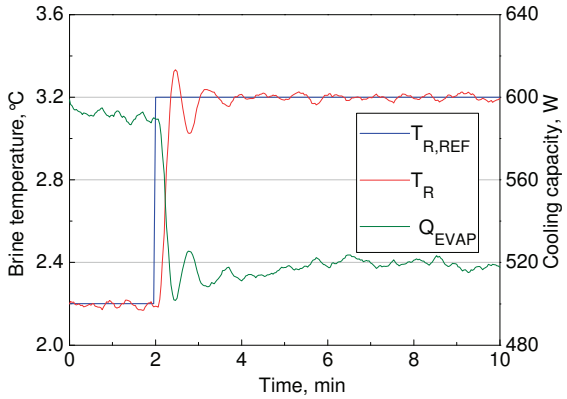

Figure 8: T_R - reference tracking

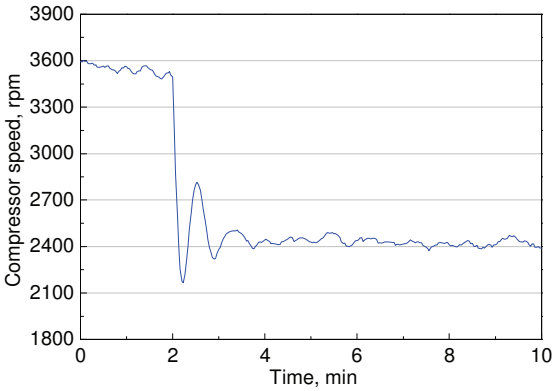

Figure 9: N_{COMP} - control action

It is worth noting that an increase in $T_{R,REF}$ is accompanied by a drop in N_{COMP} and Q_{EVAP}. This is a clear indication that the cooling capacity can be indirectly controlled by the brine exit temperature. It can also be seen that the controller worked as expected, with an overshoot of 25% and with a settling time of 60s.

5. Dual SISO CONTROLLER

The dual SISO control strategy was derived from the two individual controllers, as illustrated in the block diagram of Figure 10. This allowed the simultaneous control of T_R and T_{SH}, to match the thermal load with the cooling capacity at the maximum *COP* value.

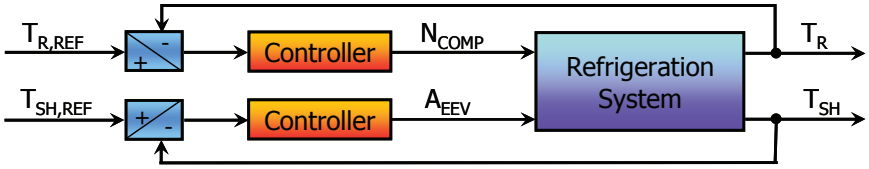

Figure 10: The dual SISO controller

5.1. Dual SISO - superheat tracking

The integrated controller was firstly evaluated by considering the standard conditions at the beginning of the test, a reference brine exit temperature ($T_{R,REF}$) of 2.2°C and a $T_{SH,REF}$ step change of 14.3°C to 12°C. Figures 11 to 14 show the T_{SH} and T_R time evolutions and also the controller action on A_{EEV} and N_{COMP} when $T_{SH,REF}$ was changed.

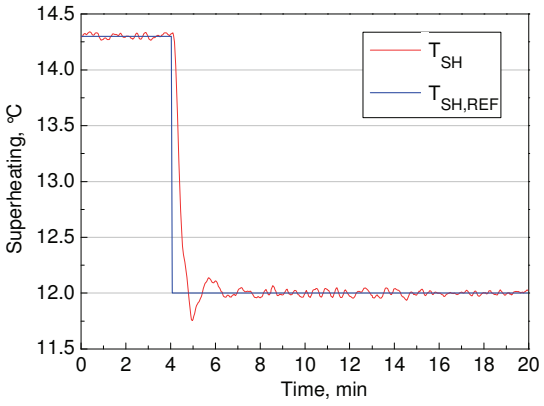

Figure 11: T_{SH} reference tracking

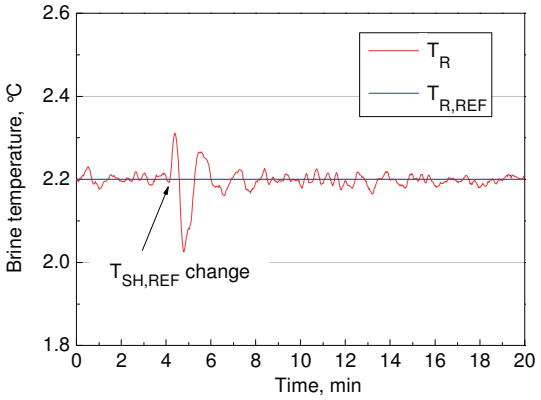

Figure 12: $T_{R,REF}$ constant

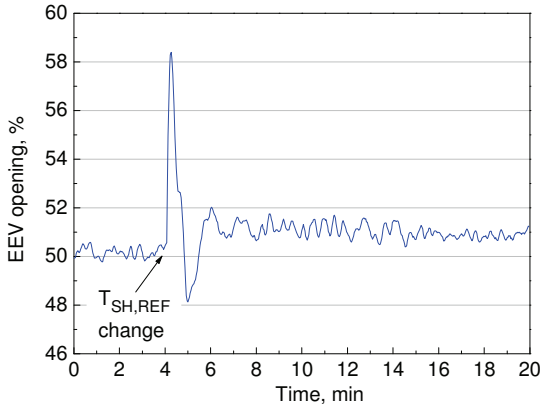

Figure 13: A_{EEV} controller

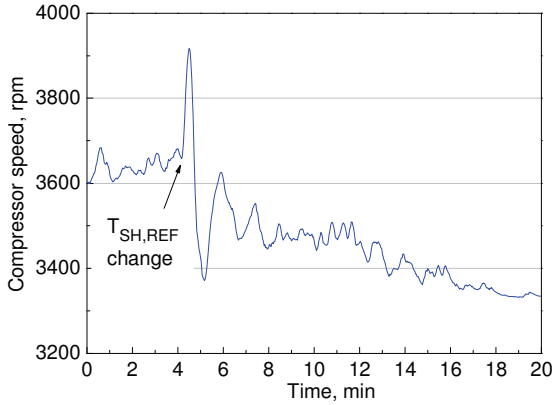

Figure 14: N_{COMP} controller

It can be observed that the controller maintained T_R at 2.2°C and T_{SH} at 12°C, by increasing A_{EEV} (50% to 51%) and reducing N_{COMP} (3650rpm to 3350rpm). In this case the T_{SH} settling time and overshoot reached values of 120s and 10%, respectively. The cooling capacity was kept constant at 592W, even with a $T_{SH,REF}$ change, since the brine exit temperature did not change.

Tests were also carried out in an attempt to identity the T_{SH} value that maximizes the system *COP*. Figure 15 shows the *COP* and Q_{EVAP} steady-state behavior as a function of $T_{SH,\,REF}$. It can be noted that the *COP* reached a maximum when the $T_{SH,\,REF}$ values were within the range of 6°C to 8°C. The corresponding control actions on A_{EEV} and N_{COMP} are shown in Figure 16. Figure 15 shows that the cooling capacity remained constant, independently of the $T_{SH,REF}$ value.

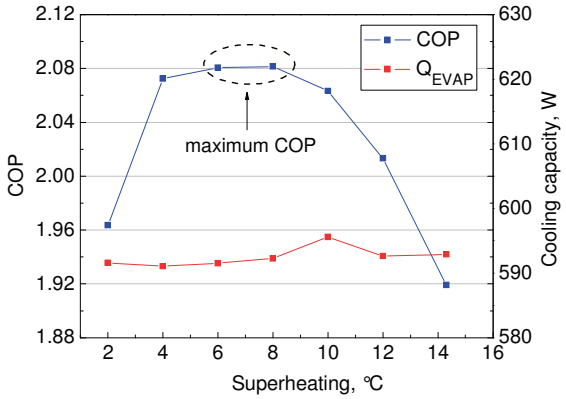

Figure 15: *COP* and Q_{EVAP}

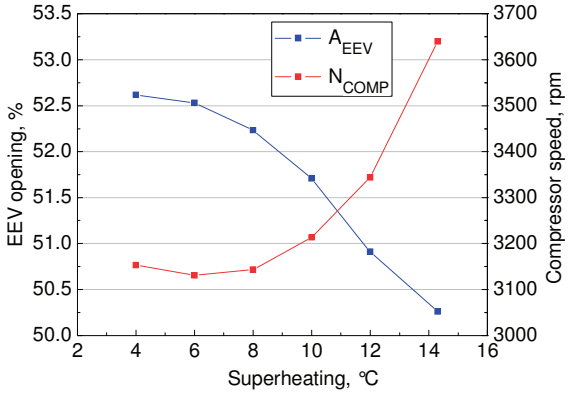

Figure 16: N_{COMP} and A_{EEV}

5.2. Dual SISO - disturbance rejection

The performance of the dual SISO control strategy regarding disturbance rejections was evaluated by changing the brine volumetric flow rate ($V_{B,EVAP}$) from 1.18L/min to 1.41L/min. The volumetric flow rate change, and thus the evaporator heat transfer rate disturbance, was detected automatically by the controller that increased N_{COMP} from 2830rpm to 4020rpm and A_{EEV} from 52.9% to 59.0%, in order to maintain T_R at 2.5°C and T_{SH} at 6°C, as shown in Figures 17 to 19. These changes increased the cooling capacity from 562W to 673W (Figure 20).

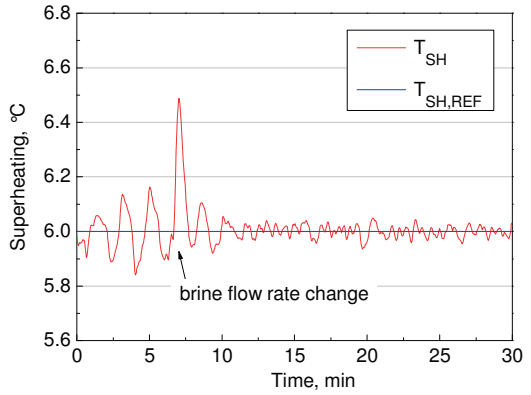

Figure 17: Disturbance rejection - T_{SH}

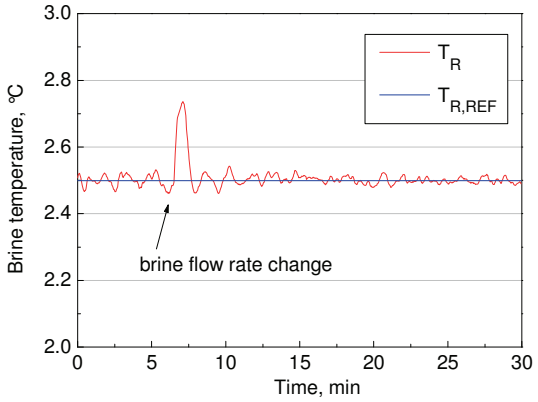

Figure 18: Disturbance rejection - T_R

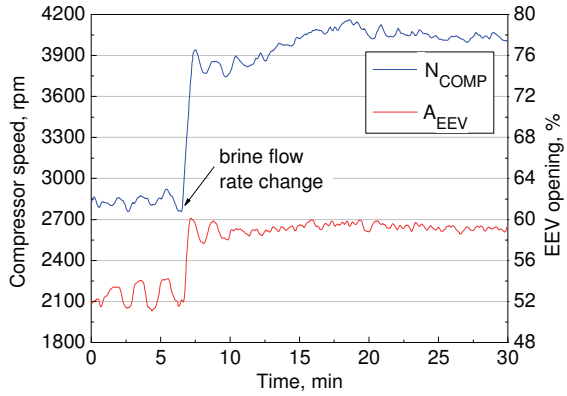

Figure 19: Disturbance rejection - N_{COMP} and A_{EEV}

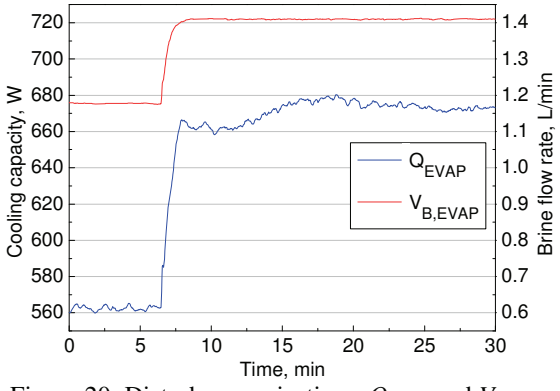

Figure 20: Disturbance rejection - Q_{EVAP} and $V_{B,EVAP}$

Figure 21 shows the steady-state values of N_{COMP} and A_{EEV}, for three different cooling capacities within a range of

450W to 675W. The experimental apparatus was run under the standard conditions with the T_R and T_{SH} parameters set at 2.5°C and 6.0°C, respectively (see Figure 22). The results showed that despite being very simple, the adopted control strategy kept the experimental apparatus running at a point of maximum performance.

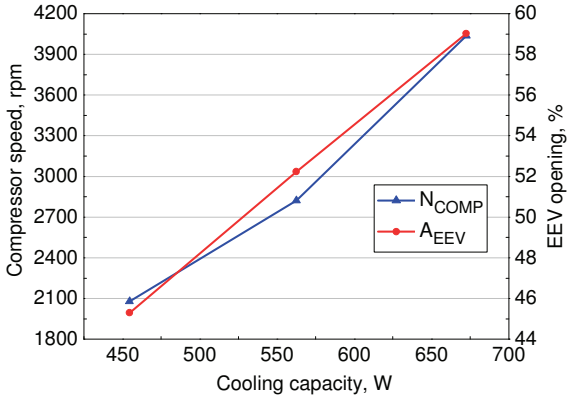

Figure 21: N_{COMP} and A_{EEV} - different cooling capacity

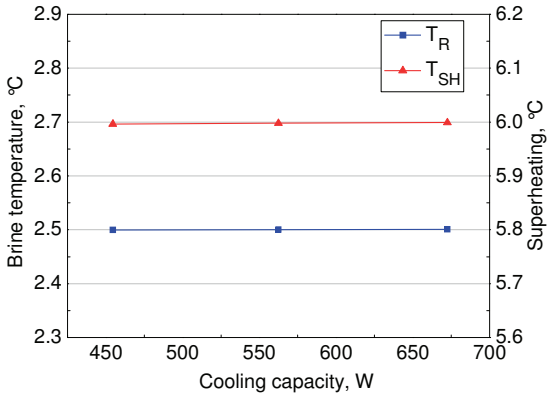

Figure 22: T_R and T_{SH} - different cooling capacity

CONCLUDING REMARKS

Two independent controllers acting on the expansion valve opening and compressor speed were designed and used to control an experimental refrigeration loop. Both controllers showed a satisfactory performance for reference tracking of the superheating degree and brine exit temperature. The two controllers were integrated through a dual SISO strategy in order to control the two variables simultaneously. The strategy proved to be a simple and effective way of controlling the cooling capacity while maintaining the system COP at its maximum value.

REFERENCES

Hong, W., Granryd, E., Kraft, H., 1992, A Pulse Width Modulation Control System for Regulating Refrigerant Flow into an Evaporator, *Singapore International Conference on Intelligent Control and Instrumentation*, pp. 603-607.

Outtagarts, A.; Haperschill, P.; Lallemand, M., 1997, The Transient Response of an Evaporator Fed Through an Electronic Expansion Valve, *Int. Journal of Energy Research*, Vol. 21, pp. 793-807

Pottker, G., Melo, C., 2007, Experimental Study of the Combined Effect of the Refrigerant Charge, Compressor Speed and Expansion Valve Opening in a Refrigeration System, *22nd IIR International Congress of Refrigeration*, Beijing.

Shimma, Y., Tateuchi, T., Sugiura, H., 1988, Inverter Control Systems in a Residential Heat Pump Air Conditioner, *ASHRAE Transactions*, Paper HI-85-31, pp. 1541-1552.

Tassou, S. A., Qureshi, T. Q., 1996, Review Paper - Variable-Speed Capacity Control in Refrigeration Systems, *Applied Thermal Engineering*, Vol. 16(2), pp. 103-113.

Ziegler, J.G., Nichols, N.B., 1942, Optimum Settings for Automatic Controllers, *Trans. of the A.S.M.E. 64*, pp. 759-768.

ACKNOWLEDGEMENTS

The authors are grateful to *Empresa Brasileira de Compressores* (Embraco S. A.) for sponsoring this research program and for technical discussions. The continued support for this research program from *Financiadora de Estudos e Projetos* (FINEP) is also duly acknowledged.